Recent Advances in Mechatronics

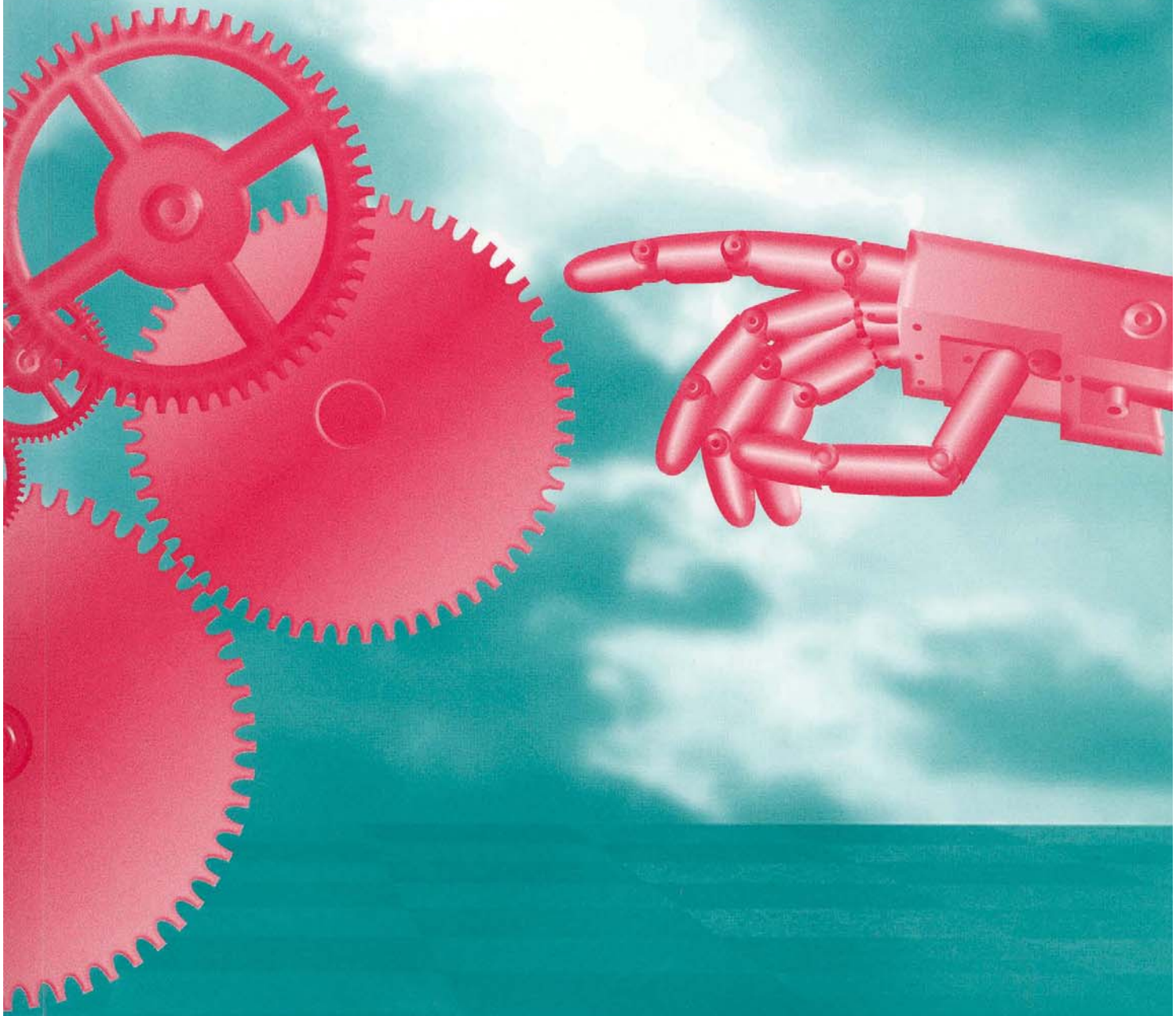

Okyay Kaynak
Sabri Tosunoglu
Marcelo Ang, Jr
(Eds.)

Springer

Chaotic Phenomena and Performance Optimization in the Trajectory Control of Redundant Manipulators

Fernando B. M. Duarte[1], J. A.Tenreiro Machado[2]

[1]Escola Superior de Tecnologia Viseu, Dep. Matemática,
Campus Politécnico, 3510 Viseu, Portugal
Email:fduarte@mat.estv.ipv.pt
[2]Instituto Superior de Engenharia do Porto
Dep. de Eng. Electrotécnica, Portugal
Email: jtm@dee.isep.ipp.pt

Abstract - Redundant manipulators have some advantages when compared with classical arms because they allow the trajectory optimization, both on the free space and on the presence of obstacles, and the resolution of singularities. For this type of manipulators, several kinematic control algorithms adopt generalized inverse matrices. In this line of thought, the generalized inverse control scheme is tested through several experiments that reveal the difficulties that often arise. Motivated by these problems this paper presents a new method that optimizes the manipulability through a least square polynomial approximation to determine the joints positions. Moreover, the article studies the chaos revealed by the kinematics trajectory planning scheme, as well as its influence on the dynamics, when controlling redundant and hyper-redundant manipulators. The experiment confirm the superior performance of the proposed algorithm for redundant and hyper-redundant manipulators, revealing several fundamental properties of the chaotic phenomena, and gives a deeper insight towards the future development of superior trajectory control algorithms.

1. Introduction

A kinematically redundant manipulator is a robotic arm possessing more degrees of freedom (*dof*) than those required to establish an arbitrary position and orientation of the end effector. Redundant manipulators offer several potential advantages over non-redundant arms. In a workspace with obstacles, the extra *dof* can be used to move around or between obstacles and thereby to manipulate in situations that otherwise would be inaccessible [1, 2, 4].

When a manipulator is redundant, it is anticipated that the inverse kinematics admits an infinite number of solutions. This implies that, for a given location of the manipulator's end effector, it is possible to induce a self-motion of the structure without changing the location of the gripper. Thus, the arm can be reconfigured to find better postures for an assigned set of task requirements.

Many techniques for solving the kinematics of redundant manipulators that have been suggested control the end effector indirectly, through the rates at which the joints are driven, using the pseudoinverse of the Jacobian [3]. Nevertheless, these algorithms lead to a kind of chaotic motion with unpredictable arm configurations. Therefore, an

important area of research remains open and more efficient algorithms must be envisaged.
Having these ideas in mind, the paper is organized as follows. Section 2 develops kinematics and dynamics of redundant manipulators. Based on these concepts, section 3 presents several experiments with the kinematics and dynamics of different redundant robots. The results reveal a chaotic behavior that is further analyzed in section 4. Finally, section 5 draws the main conclusions.

2. Kinematics and Dynamics of Redundant Manipulators

2.1 Problem Formulation

We consider a manipulator with *n dof* whose joint variables are denoted by $\mathbf{q} = [q_1, q_2, ..., q_n]^T$. We assume that a class of tasks we are interested in can be described by m variables, $\mathbf{x} = [x_1, x_2, ..., x_m]^T$ ($m < n$) and that the relation between $\mathbf{q}$ and $\mathbf{x}$ is given by:

$$\mathbf{x} = f(\mathbf{q}) \tag{1}$$

where f is a function representing the direct kinematics. Differentiating (1) with respect to time yields:

$$\dot{\mathbf{x}} = \mathbf{J}(\mathbf{q})\dot{\mathbf{q}} \tag{2}$$

where $\dot{\mathbf{x}} \in \Re^m$, $\dot{\mathbf{q}} \in \Re^n$ and $\mathbf{J}(\mathbf{q}) = \partial f(\mathbf{q})/\partial \mathbf{q} \in \Re^{m \times n}$.

Several approaches for solving redundancy that have been proposed [5, 8] are based on the inversion of equation (2). A solution in terms of the joint velocities, is sought as

$$\dot{\mathbf{q}} = \mathbf{J}^{\#}(\mathbf{q})\dot{\mathbf{x}} \tag{3}$$

where $\mathbf{J}^{\#}$ is one of the generalized inverses [6] of the $\mathbf{J}$.

A direct consequence is that it is possible to generate internal motions that reconfigure the manipulator structure without changing the gripper position and orientation [7, 9]. Another aspect revealed by the solution of (3) is that repetitive trajectories in the operational space do not lead to periodic trajectories in the joint space. This is an obstacle for the solution of many tasks because the resultant robot configurations have similarities with those of an chaotic system.
In order to solve this lack of repetition we adopt a distinct approach, entitled Open-Loop Manipulability (OLM) optimization method [10]. For a given point (x,y) in the operational space the new algorithm consists on computing the point in the joint space that maximizes the manipulability index $\mu = \sqrt{\det\left(\mathbf{J}\mathbf{J}^T\right)}$. Given the symmetry of the robot kinematics, μ_{max}, the maximum value of μ, just depends on the radial distance $r = \sqrt{x^2 + y^2}$ of the point from the origin of coordinates and, therefore, we get the set of $n-m$ joint positions $q_j(r)$, ..., $q_{j+n-m}(r)$ optimal in a μ perspective. From these values

and using a standard least squares method we calculate $n-m$ polynomials that fit approximately the data. Once fixed these variables, the other m joint positions can be calculate through a standard inverse kinematic algorithm.
The numerical calculation of the maximum manipulability (μ_{max}) and the corresponding joint values increase with the number of *dof*, but they can be computed off-line without imposing an high load to real-time control systems.

2.2 Kinematics of Planar Redundant Manipulators

The direct kinematics and the Jacobian of a k-link manipulator has a simple recursive nature according with the expressions:

$$\begin{bmatrix} x \\ y \end{bmatrix} = \begin{bmatrix} l_1C_1 + l_2C_{12} + l_3C_{123} + \cdots + l_kC_{12\ldots k} \\ l_1S_1 + l_2S_{12} + l_3S_{123} + \cdots + l_kS_{12\ldots k} \end{bmatrix} \tag{5.a}$$

$$\mathbf{J} = \begin{bmatrix} -l_1S_1 - l_2S_{12} - \cdots - l_kS_{1\ldots k} & \cdots & -l_kS_{1\ldots k} \\ l_1C_1 + l_2C_{12} + \cdots + l_kC_{1\ldots k} & \cdots & l_kC_{1\ldots k} \end{bmatrix} \tag{5.b}$$

where l_i is the length of link i, $S_{i\ldots k} = Sin(q_i + \cdots + q_k)$ and $C_{i\ldots k} = Cos(q_i + \cdots + q_k)$.
During the experiments, for all manipulators, it is considered $\Delta t = 0.001\text{sec}$, $l_1 + l_2 + l_3 \ldots + l_k = 3$ and $l_1 = l_2 = l_3 \ldots = l_k$.
In the closed-loop pseudoinverse's method (CLP) the joint positions can be computed through the time integration of the velocities (3) according with the block diagram of the inverse kinematics algorithm depicted in Figure 1.

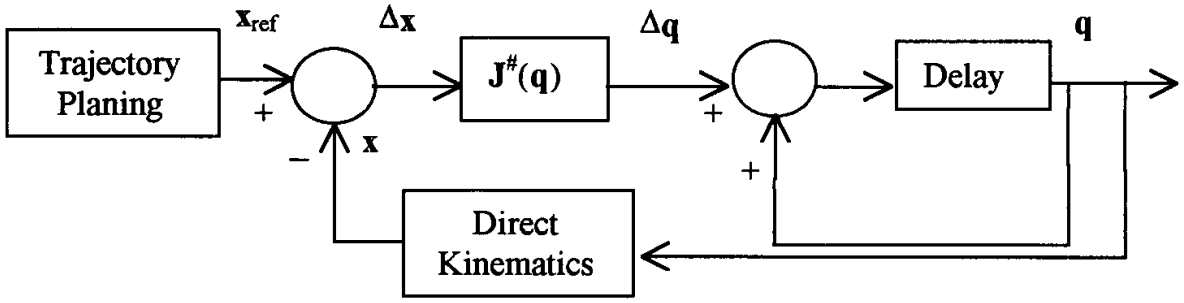

Fig. 1: Block diagram of the closed-loop inverse kinematics algorithm with the pseudoinverse.

2.3 Dynamics of Planar Redundant Manipulators

The symbolic formulae for the inverse dynamics of a k-link planar manipulator can be also formulated recursively as:

$$
\begin{aligned}
T_i = & \sum_{i=1}^{n}(m_i(\sum_{p=1}^{i-1}(If\,[j>p, B1=0, B1=1]\}, l_p{}^2\sum_{u=1}^{p}\ddot{q}_u B1) \\
& + r_i{}^2\sum_{u=1}^{i}\ddot{q}_u + \sum_{p=2}^{i}(\sum_{k=1}^{p-1}(If\,[p>i-1, B2=0, B2=1]\}, \\
& [If\,[p==i, B3=1, B3=0]], If\,[j>k, B4=0, B4=1]\}, \\
& If\,[(j>=k+1\&\&j<=p), B5=1, B5=0]\}, \\
& l_k(l_p B2 + r_p B3)((-S_{k+1..p}((\sum_{u=k+1}^{p}\dot{q}_u)^2 + \\
& 2\sum_{u=1}^{k}\dot{q}_u\sum_{u=k+1}^{p}\dot{q}_u) + C_{k+1..p}(\sum_{u=1}^{p}\ddot{q}_u + \sum_{u=1}^{k}q_u)))B4 + \\
& (S_{k+1..p}(\sum_{u=1}^{k}\dot{q}_u)^2 + C_{k+1..p}\sum_{u=1}^{k}\ddot{q}_u)B5 + \\
& g(\sum_{p=1}^{i-1}(If\,[j>p, B1=0, B1=1]\}, l_p C_{1..p} B1) + r_i C_{1..i})))
\end{aligned}
\tag{6}
$$

where T_i are the joint torques, B1 to B5 are logical conditions, m_i is the mass of link i, r_i is the distance from the joint axis to the link center of mass and g is the acceleration due to gravity.

3. Trajectory Control of Redundant and Hyper-Redundant Robots

In this sections we analyze for different manipulators the performances of the trajectory controllers based on the CLP and OLM methods. In this line of thought, we study the joint trajectories for the planar redundant $3R$ and the planar hyper-redundant $4R$ robot, when subjected to a repetitive circular trajectory in the operational space with radius R.

3.1 Planar Redundant Manipulators

In this experiment we adopt the $3R$ arm with an initial posture $\mathbf{q}(0) = [\pi \quad -\pi/2 \quad -\pi/2]^T$. Figure 2 shows the joint positions using the CLP method. In an alternative experiment, Figure 3 shows the joint positions the OLM method. In this case, it is adopted the least square approximation polynomial $q_3 = 0.51r - 2.09$ for joint 3.

In these two experiments we have distinct results. When adopting the CLP, the manipulability is non-optimal and the joint trajectories exhibit sudden changes, which impose large joint velocities. Moreover, the joint trajectories are non-repetitive leading to a kind of chaotic performance. When using the OLM procedure the trajectory is repetitive without large or fast transients.

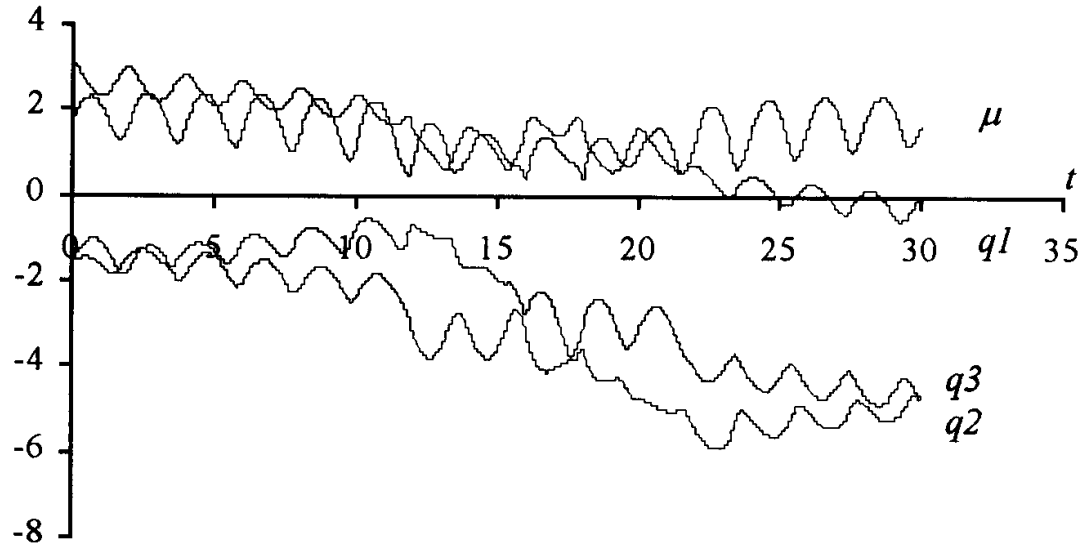

Fig. 2: The 3*R*-robot joint positions *versus* time using the CLP method.

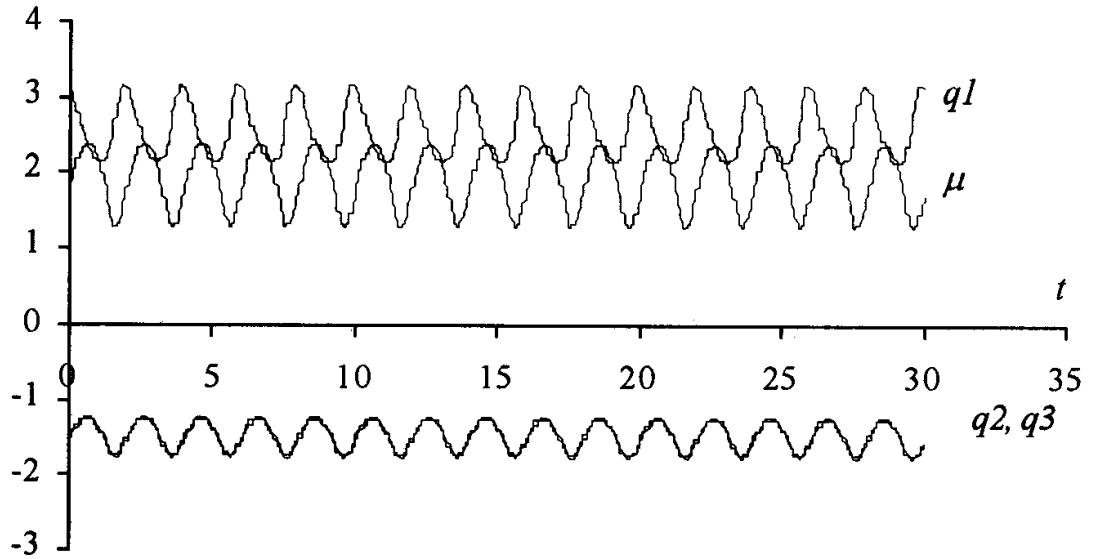

Fig. 3: The 3*R*-robot joint positions *versus* time using the OLM method.

3.2 Planar Hyper-Redundant Manipulators

In this sub-section we consider the planar 4*R* hyper-redundant manipulator under the control of the two previous methods. In the CLP method the manipulators initial configurations are: $\mathbf{q}(0)=[0.97\pi \;\; -0.28\pi \;\; -0.41\pi \;\; -0.39\pi]^T$. In the OLM algorithm we adopt least squares polynomial approximations. For joints 3 and 4 of the 4*R*-robot we use: $q_3 = 0.41r^2 - 0.60r - 1.62$ and $q_4 = -0.24r^2 + 1.13r - 1.78$.

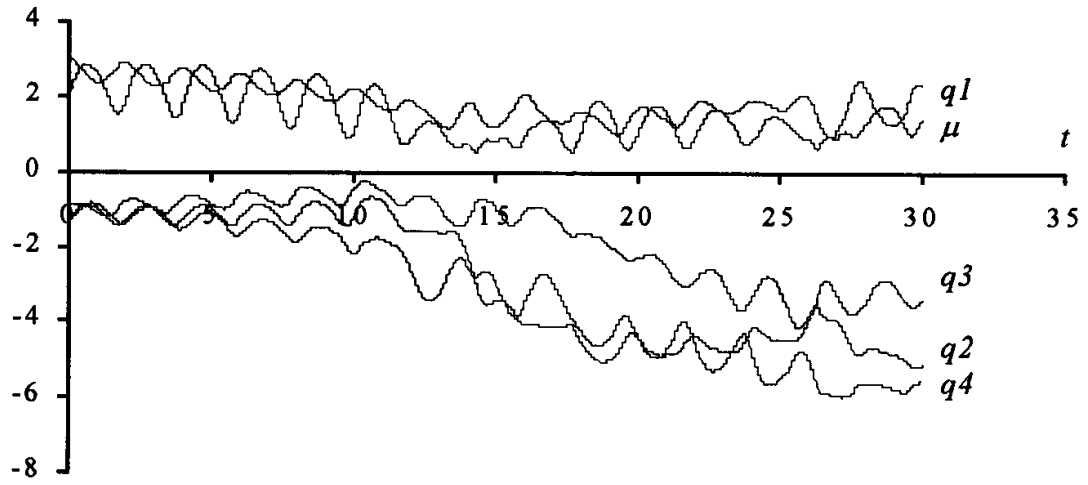

Fig. 4: The 4*R*-robot joint positions *versus* time using the CLP method.

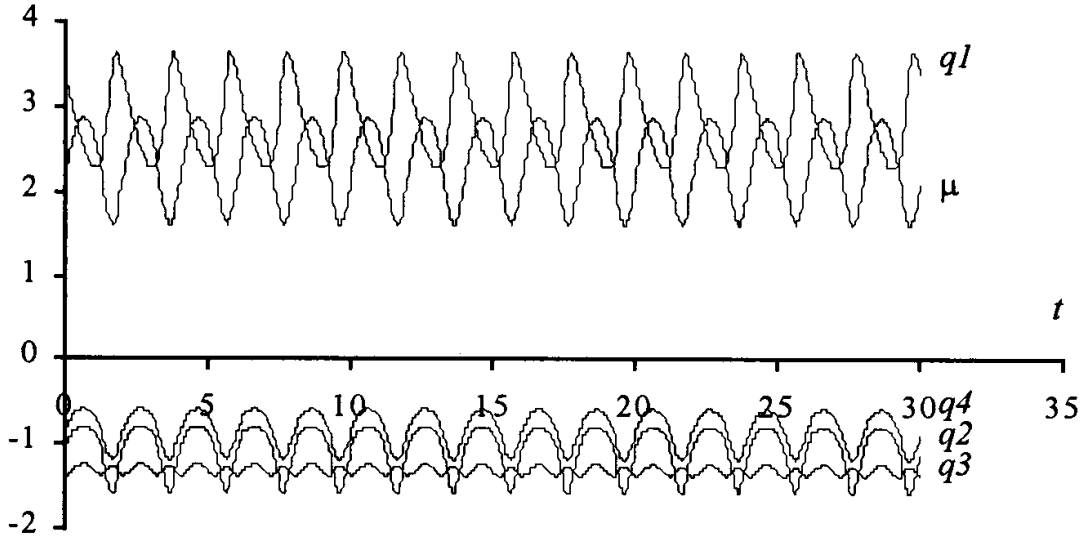

Fig. 5: The 4*R*-robot joint positions *versus* time using the OLM method.

In these experiments (Figs. 4 to 5) we observe performances similar to those revealed by the 3*R*-robot. Moreover, for the proposed method, the manipulability index μ seems to show better performances the higher the number of robot *dof*.
This conclusion is consistent with the fact that the larger the number of *dof* the higher the manipulability (for the appropriate robot configuration) as can be seen in Figure 6. Therefore, the OLM method taker advantage of this property while the CLP algorithm spans a large range of sub-optimal manipulability configurations.

In a second set of experiments we analyze the robot inverse dynamics when subjected to the repetitive circular trajectory in the operational space. Figure 7 and Figure 8 shows the resulting the joint torque for the planar 3*R* manipulator under the CLP and OLM

methods. It is clear that, under the CLP method, the dynamics follows the kinematic non-repetitive responses and, therefore, exhibits the same type of problems.

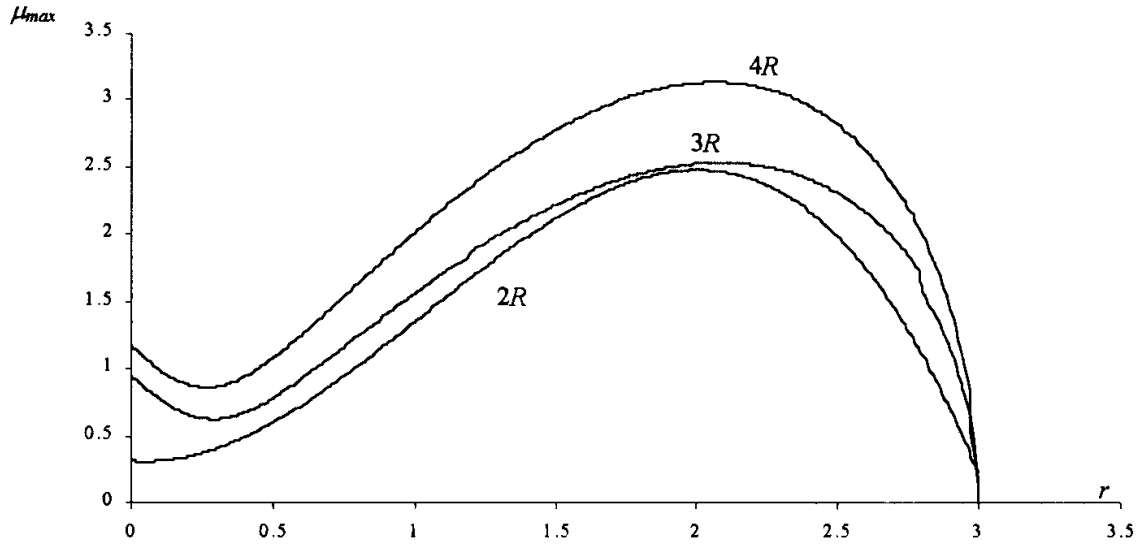

Fig. 6: Maximum manipulability μ_{max} *versus* the radial distance r for the $2R$, $3R$ and $4R$ robots.

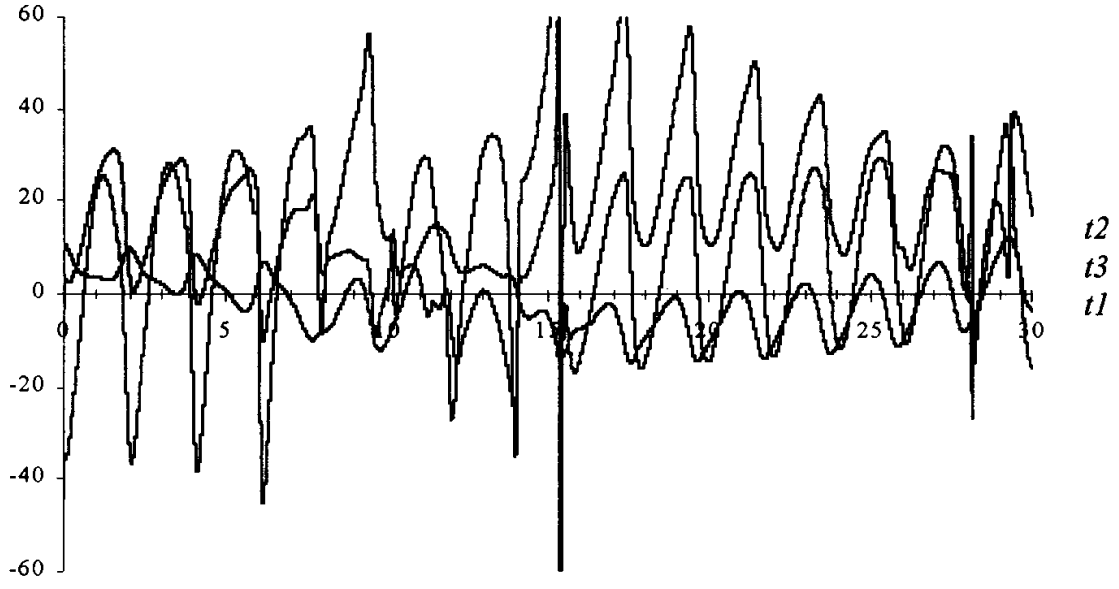

Fig. 7: The $3R$-robot joint torque *versus* time using the CLP method (R = 0.5). At *t=15.3 sec* there is a chart pick, for joint 1 torque, with a maximum value t_1=158.1. The maximum for joint 2 torque is t_2=67.6 at *t=15.3 sec* and the maximum for joint 3 torque is t_3=14.7 at *t=11.57 sec*.

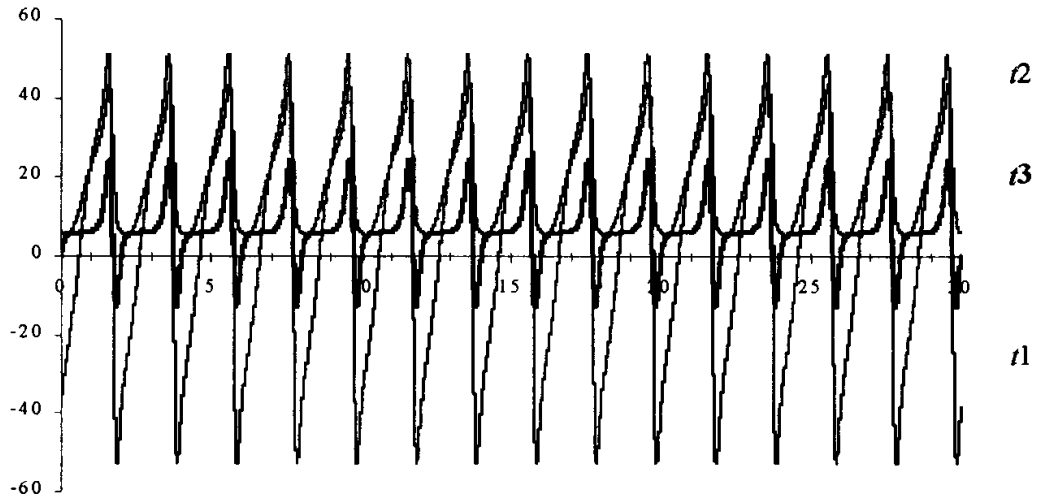

Fig. 8: The 3*R*-robot joint torque *versus* time using the OLM method (R = 0.5).

4. On the Chaotic Responses of the Pseudoinverse Algorithm

It was shown previously that the pseudoinverse algorithm leads to unpredictable arm configurations, with responses similar to those of a chaotic system [12, 13].
For example, Figure 11 and Figure 12 depict the phase-plane trajectories for joint 1 of the planar 3*R*-robot kinematics and dynamics, respectively, when repeating a circular motion with center at r = 1 and radius R = 0.1. Besides the position and velocity drifts, leading to different trajectory loops, we have points that are 'avoided'. Such points correspond to arm configurations where several links are aligned. This characteristic is inherent to the pseudoinverse matrix because the planar 3*R*-robot was tested both under open-loop and closed-loop control, leading to the same type of behavior. In order to gain further insight into the pseudoinverse chaotic nature, the robots under investigation were required to follow the cartesian repetitive circular motion for several radial distances r. The phase-plane joint trajectories were then analyzed and their fractal dimension *dim* estimated through the standard box-counting method [11]:

$$\dim S = \lim_{\varepsilon \to 0} \frac{\ln N(\varepsilon)}{\ln (1/\varepsilon)} \tag{7}$$

where $N(\varepsilon)$ denotes the smallest number of bi-dimensional boxes of side length ε required in order to completely cover the plot surface.
Figure 20 shows the resulting chart revealing that:

- for the pseudoinverse method we have *dim* $\approx$ 2 due to the position and velocity drifts, in contrast with the case for the 2*R* where we have *dim* = 1.
- the fractal dimension diminishes near the maximum radial distance (*i.e.* r = 3).
- for each type of robot the fractal dimension is nearly the same, for all joints.

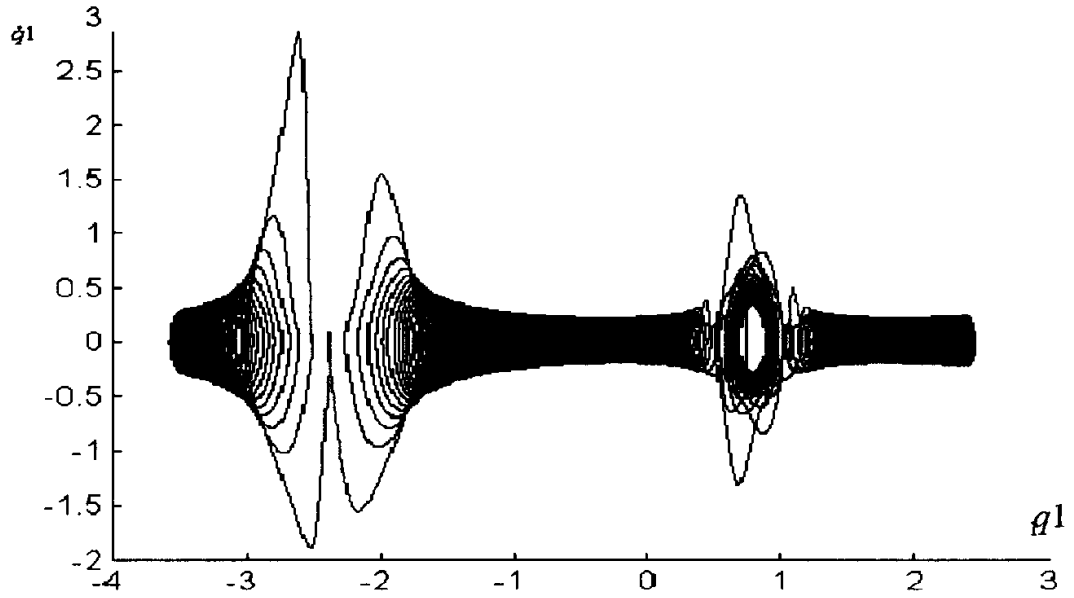

Fig. 9: Phase plane trajectory for the 3*R*- robot - joint 1 at $r = 1, R = 0.1$, *dim* = 1.62.

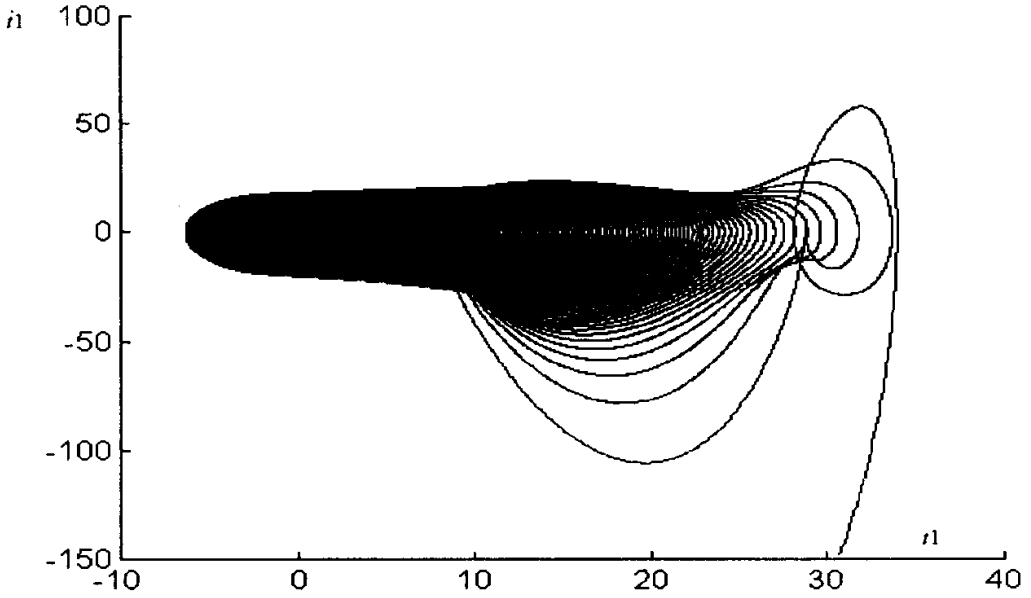

Fig. 10: Phase plane trajectory for the 3*R*- robot - torque 1 at $r = 1, R = 0.1$, *dim* = 1.69.

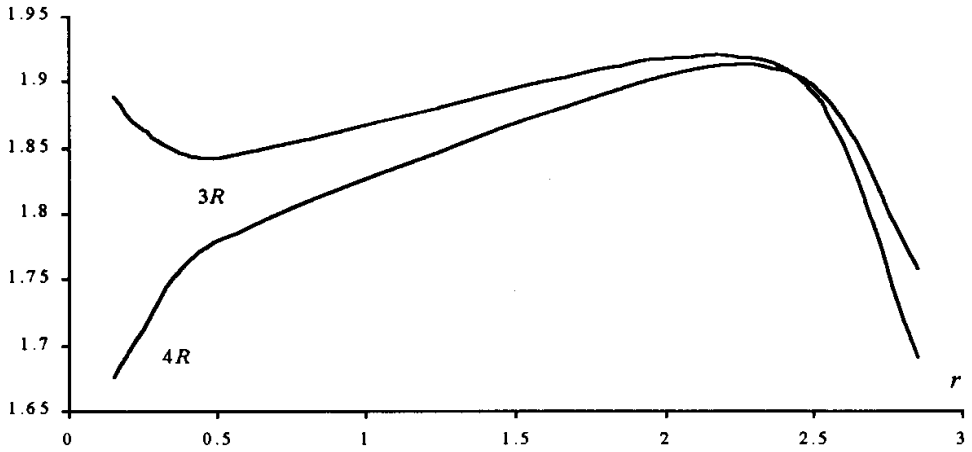

Fig. 11: Fractal dimension *dim* of the kinematic phase-plane *versus* the radial distance *r* for the 3*R* and 4*R* robots, $R = 0.1$.

The robot chaotic motion is due to the uncontrolled contribution of the Jacobian pseudoinverse to the manipulator inner motion. Nevertheless, a deeper insight into the nature of this motion must be envisaged. Therefore, two distinct experiments were devised in order to establish the texture of the Jacobian null space.

In a first set of experiments with the CLP scheme, the robot is required to follow circular motions in the operational space with fixed center but different radius R. The resulting charts of the robot joint velocities, after several cycles are then approximated, numerically, through a Fourier series.

The constant term for the velocity series approximation is, in fact, the term responsible for the drift in the phase plane charts depicted previously. The results reveal that the amplitude of the velocity drift is 'induced' by the amplitude of the circle radius. The corresponding analytical relationship is of the type $\dot{q}_i \sim R^{\alpha}$ (i = 1,2,3) with $1.9 < \alpha < 3.2$ and, therefore, the higher the amplitude of R the more serious becomes the robot chaotic response.

In a second experiment, the robot to starts in an initial random configuration with $q_i \in]-\pi,\pi]$ (i = 1, 2, 3) and is required to attain a fixed point in the operational space under the control of the CLP scheme. After elapsing the trajectory transient, the final robot joint positions are recorded. The experiment is repeated in order to establish a statistical characterization of the manipulator steady-state configuration. Figure 12 shows a typical histogram for the planar 3R robot joint positions. For a given desired position in the operational space, we conclude that the possible robot configurations have distinct probabilities. In this perspective, Figure 13 shows the variation of the most probable q_i (i = 1, 2, 3) *versus* the radial distance r (with $x = r$ and $y = 0$).

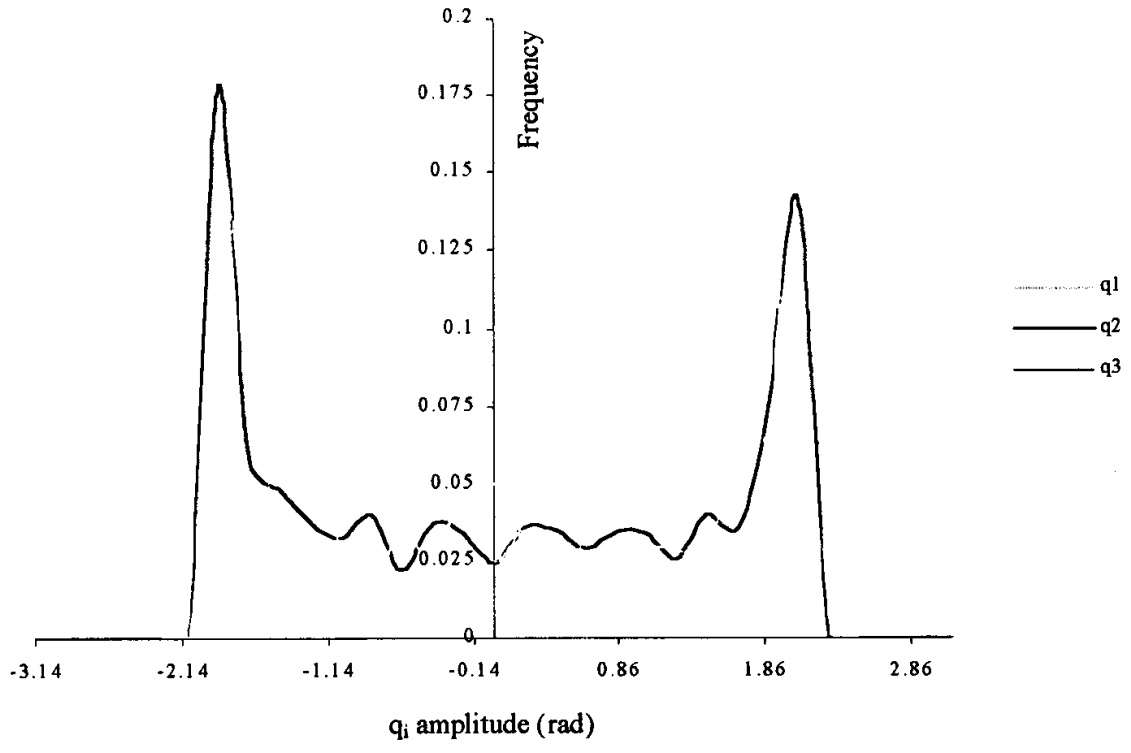

Fig. 12: Histogram for the 3R robot joint positions for the operating point $(x, y) = (\sqrt{2}, \sqrt{2})$.

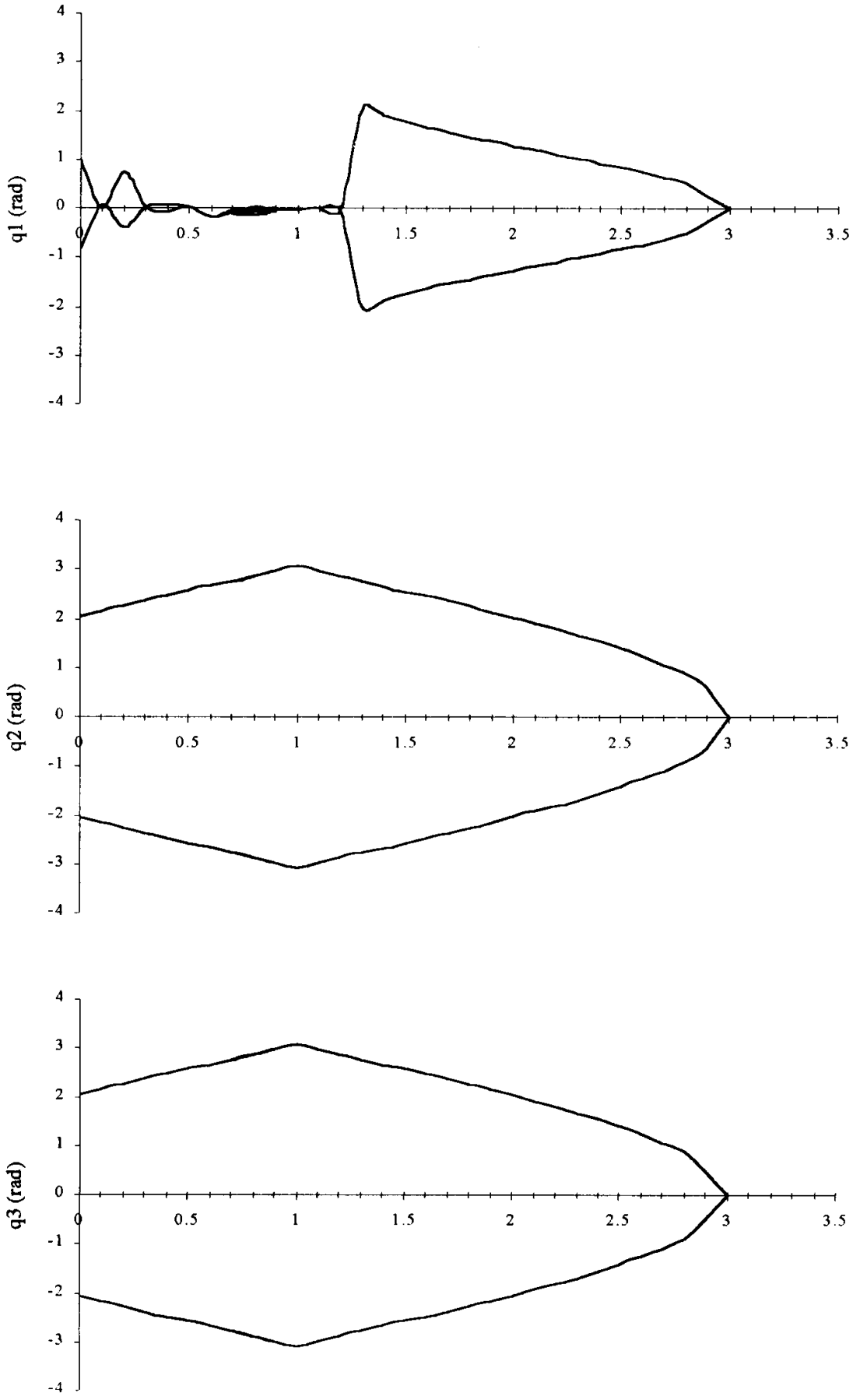

Fig. 13: Most probable robot joint positions *versus* the radial distance *r*.

5. Conclusions

This paper discussed several aspects of the chaotic phenomena generated by the pseudoinverse-based trajectory control of redundant manipulators. Furthermore, the study addressed both the kinematics and dynamics in order to test the influence of each model. In this perspective, the fractal dimension of the responses was analyzed showing that it is independent of the robot joint. In fact, the chaotic motion depends solely on the operational space point and on the amplitude of the exciting repetitive motion. Moreover, a second group of experiments reveals that the robot inner motion, that spans the null space of the Jacobian matrix, leads to 'preferred' configurations while avoiding other areas. Nevertheless, the relationship between the fractal dimension of the phase plane portraits, the amplitude of the exciting repetitive signal and the statistics of the robot joint configurations is not completely clear and further research on this aspects needs still to be done in order to develop superior trajectory planning algorithms.

References

1 E. Sahin Conkur, And Rob Buckingham "Clarifying the Definition of Redundancy as Used in Robotics", *Robotica*, vol. 15, pp. 583-586, 1997.

2 Stefano Chiaverini "Singularity-Robust task-Priority Redundancy Resolution for Real Time Kinematic Control of Robot Manipulators", *IEEE Trans. Robotics Automation*, vol. 13, pp. 398-410, 1997.

3 C.A Klein, and C. C Huang, "Review of Pseudoinverse Control for Use With Kinematically Redundant Manipulators", *IEEE Trans. Syst. Man, Cyber.*, vol. 13, pp. 245-250, 1983.

4 Yoshikawa, T., "*Foundations of Robotics: Analysis and Control*", MIT Press, 1988.

5 Y. Nakamura, "*Advanced Robotics: Redundancy and Optimization*", Addinson-Wesley, 1991.

6 Keith L. Doty, C. Melchiorri and C. Bonivento, "A Theory of Generalized Inverses Applied to Robotics", *Int. Journal of Robotics Research*, vol. 12, pp. 1-19, 1993.

7 Bruno Siciliano, " Kinematic Control of Redundant Robot Manipulators: A Tutorial", *Journal of Intelligent and Robotic Systems*, vol. 3, pp. 201-212, 1990.

8 W.J.Chung, Y. Youm and W. K. Chung, "Inverse Kinematics of Planar Redundant Manipulators via Virtual Links With Configuration Index", *J. of Robotic Systems*, vol. 11, pp. 117-128, 1994.

9 Sanjeev Seereeram and John T. Wen, "A Global Approach to Path Planning for Redundant Manipulators", *IEEE Trans. Robotics Automation*, vol. 11, pp.152-159, 1995.

10 Fernando B.M. Duarte and J.A. Tenreiro Machado, "Kinematic Optimazition of Redundant and Hyper-Redundant Robot Trajectories", ICECS'98-5th IEEE Int. Conference on Electronics, Circuits and Systems, Lisbon, Portugal, 1998.

11 James Theiler, "*Estimating Fractal Dimension*", *Journal Optical Society of America*, vol. 7, n°6, pp. 1055-1073, 1990.

12 J.A.Tenreiro Machado and Fernando B. Duarte, "Redundancy Optimization for Mechanical Manipulators", *AMC'98*-5th IEEE Int. Workshop on Advanced Motion Control, Coimbra, Portugal, 1998.

13 Fernando B. Duarte and J.A. Tenreiro Machado, "On the Optimal Configuration of Redundant Manipulators", INES'98- 9th IEEE Int. Conf. on Intelligent Engineering Systems, Vienna, Austria, 1998.